Inorganic Chemistry
Article

Inorg. Chem. **2010**, *49*, 3441–3448 **3441**
DOI: 10.1021/ic902527e

Mixed Alkali Metal/Transition Metal Coordination Polymers with the Mellitic Acid Hexaanion: 2-Dimensional Hexagonal Magnetic Nets

Simon M. Humphrey,*,† Richard A. Mole,‡ Richard I. Thompson,§ and Paul T. Wood*,§

†*Department of Chemistry and Biochemistry, The University of Texas at Austin, 1 University Station A5300, Austin, Texas 78712,* ‡*Forschungsneutronenquelle Heinz Maier-Leibnitz (FRM II), Technische Universität München, Lichtenbergstrasse 1, 85747 Garching, Germany, and* §*University Chemical Laboratory, University of Cambridge, Lensfield Road, Cambridge CB2 1EW, U.K.*

Received December 18, 2009

The hexaanion of mellitic acid, mel = $(C_6(CO_2)_6)^{6-}$, links metal ions into extensively connected magnetic coordination polymers. Reaction of alkali metal mellitate salts, M_6(mel) (M = K, Rb), with $M'Cl_2$ precursors (M′ = Mn, Co, Ni) under mild (473 K) hydrothermal conditions yields an extensive family of isostructural 3-dimensional mixed alkali metal/transition metal polymers of general formula $M_2[M'_2(mel)(OH_2)_2]$ (M/M′ = K/Mn (**1a**); K/Co (**1b**); K/Ni (**1c**); Rb/Mn (**2a**); Rb/Co (**2b**); Rb/Ni (**2c**)). These materials incorporate distorted 2-dimensional magnetic hexagonal nets with a honeycomb topology that are exclusively based on metal-carboxylate-metal bridging interactions. A further isostructural alkali metal-free Co^{2+} material with NH_4^+ cations, $(NH_4)_2[Co_2(mel)(OH_2)_2]$ (**3**), produced by reaction of H_6mel with $[Co(NH_3)_6]Cl_3$ is also presented. The magnetic susceptibility data for **1a**−**c**, **2a**−**c**, and **3** are presented. The susceptibility data for the Mn(II)- and Ni(II)-containing phases have been analyzed using a simple Mean Field Theory approach, and have been modeled using a high temperature series expansion. The comparative magnetism of the Co(II) phases is also presented, and is more complicated because of significant spin−orbit coupling effects.

1. Introduction

Benzene 1,2,3,4,5,6-hexacarboxylic acid, more commonly known as mellitic acid (after the aluminum-based mineral mellite in which it was first observed[1]) is an intriguing polycarboxylate ligand for the formation of dense and highly connected coordination polymer materials.[2] In particular, mellitic acid (hereafter abbreviated as $melH_6$) is useful for the preparation of multidimensional metal-organic coordination polymers that incorporate interesting, true lower-symmetry magnetic lattices of paramagnetic metal ions.[3] A key advantage of such magnetic coordination polymer systems over more conventional (inorganic) magnetic materials is that the organic components act to isolate the low dimensional magnetic topology of interest, wherein $J_{intra} \gg J_{inter}$ resulting in a lack of long-range order.

The title compounds exhibit a honeycomb (hexagonal) magnetic lattice. This network type has also been reported to exhibit diverse magnetic properties that range from spin glass behavior,[4] spin flop transitions,[5] and Kosterlitz−Thouless behavior.[6] The observation of superconductivity[7] in 2-dimensional (2D) hexagonal systems, as well as more commonly in 2D square lattice compounds such as the

*To whom correspondence should be addressed. E-mail: smh@cm.utexas.edu (S.M.H.), ptw22@cam.ac.uk (P.T.W.).

(1) Robl, C.; Kuhs, W. F. *J. Solid State Chem.* **1991**, *92*, 101.

(2) See for example: (a) Robson, R. *Dalton Trans.* **2008**, 5113. (b) Zang, S.; Su, Y.; Zhu, H.; Meng, Q. *Inorg. Chem.* **2006**, *45*, 2972. (c) Kuc, A.; Enyashin, A.; Seifert, G. *J. Phys. Chem. B* **2007**, *111*, 8179. (d) Vagin, S.; Ott, A.; Weiss, H.-C.; Karbach, A.; Volkmer, D.; Reiger, B. *Eur. J. Inorg. Chem.* **2008**, *16*, 2601. (e) Humphrey, S. M.; Mole, R. A.; McPartlin, M.; McInnes, E. J. L.; Wood, P. T. *Inorg. Chem.* **2005**, *44*, 5981. (f) Prior, T. J.; Rosseinsky, M. J. *Chem. Commun.* **2001**, 1222. (g) Young, D. M.; Geiser, U.; Schultz, A. J.; Wang, H. H. *J. Am. Chem. Soc.* **1998**, *120*, 1331.

(3) See for example: (a) Kurmoo, M. *Chem. Soc. Rev.* **2009**, *38*, 1353. (b) Zhang, W. X.; Xue, W.; Zheng, Y. Z.; Chen, X. M. *Chem. Commun.* **2009**, *25*, 3804. (c) Yoon, J. H.; Ryu, D. W.; Kim, H. C.; Yoon, S. W.; Suh, B. J.; Hong, C. S. *Chem.—Eur. J.* **2009**, *15*, 3661. (d) Yang, H.; Chen, J. M.; Sun, J. J.; Yang, S. P.; Yu, J.; Tan, H.; Li, W. *Dalton Trans.* **2009**, *14*, 2540. (e) Livage, C.; Egger, C.; Ferey, G. *Chem. Mater.* **1999**, *11*, 1546. (f) Zhang, D. J.; Song, T. Y.; Wang, l.; Shi, J.; Xu, J. N.; Wang, Y.; Ma, K. R.; Yin, W. R.; Zhang, L. R.; Fan, Y. *Inorg. Chim. Acta* **2009**, *362*, 299. (g) Lu, Y. B.; Wang, M. S.; Zhou, W. W.; Xu, G.; Guo, G. C.; Huang, J. S. *Inorg. Chem.* **2008**, *47*, 8935. (h) Mole, R. A.; Cottrell, S. P.; Stride, J. A.; Wood, P. T. *Inorg. Chim. Acta* **2008**, *361*, 3718. (i) Zheng, Y. Z.; Xue, W.; Tong, M. L.; Chen, X. M.; Grandjean, F.; Long, G. J. *Inorg. Chem.* **2008**, *47*, 4077. (j) Huang, Y. G.; Yuan, D. Q.; Pan, L.; Jiang, F. L.; Wu, M. Y.; Zhang, X. D.; Wei, W.; Gao, Q.; Yong, J.; Li, J.; Hong, M. C. *Inorg. Chem.* **2007**, *46*, 9609. (k) Humphrey, S. M.; Wood, P. T. *J. Am. Chem. Soc.* **2004**, *126*, 13237. (l) Coronado, E.; Forment-Aliaga, A.; Galan-Mascaros, J. R.; Giminez-Saiz, C.; Gomez-Garcia, C. J.; Martinez-Ferrero, E.; Nunez, A.; Romero, F. M. *Solid State Sci.* **2003**, *5*, 917. (m) Janiak, C. *Dalton Trans.* **2003**, *14*, 2781. (n) Song, J. L.; Zhao, H. H.; Mao, J. G.; Dunbar, K. R. *Chem. Mater.* **2004**, *16*, 1884.

(4) Bieringer, M.; Greedan, J. E.; Luke, G. M. *Phys. Rev. B* **2000**, *62*, 6521.

(5) Goosens, D. J.; Studer, A. J.; Kennedy, S. J.; Hicks, T. J. *J. Phys.: Condens. Matter* **2000**, *12*, 4233.

(6) Rønnow, H. M.; Wildes, A. R.; Bramwell, S. T. *Physica B* **2000**, *276−278*, 676.

(7) Shamato, S.; Kato, T.; Ono, Y.; Miyazaki, Y.; Ohoyama, K.; Ohashi, M.; Yamaguchi, Y.; Kajitni, T. *Physica C* **1998**, *306*, 7.

Published on Web 03/05/2010

Scheme 1. (a) Mellitate Hexaanion, $(C_6(CO_2)_6)^{6-}$, mel^{6-}; (b) Representation of Adjacent in-Plane and out-of-Plane Carboxylate Groups As Encouraged to Minimize Steric Clashing to Promote Formation of 3D Coordination Materials

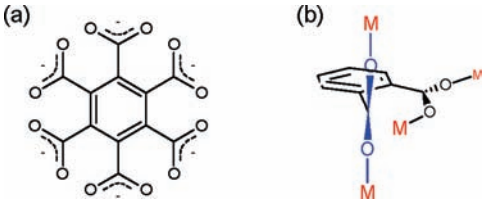

cuprates[8] and pnictides,[9] has prompted speculation that dimensionality and high temperature superconductivity are implicitly linked. In the cuprates[8] and pnictides[9] there is a strong relationship between the magnetically ordered and the superconducting phase, and in the case of the pnictides it has even been shown that the two phases coexist.[10] Aromatic carboxylates have received much attention as components in low-dimensional magnetic networks because carboxylate has the ability to mediate different types of magnetic superexchange between adjacent metal ions, based on a wide range of coordination modes that it can support.[11] Furthermore, because the formation of lower-dimensional magnetic lattices is often favored by the incorporation of anisotropic ligands, the hexaanionic hexacarboxylate, mel^{6-} is an ideal candidate (Scheme 1a). Moreover, mel^{6-} is naturally hydrogen-free and therefore magnetic materials based on mel^{6-} frameworks would be ideal candidates for neutron diffraction studies, without the requirement for (often difficult) deuteration of organic precursors.[12]

It is therefore perhaps somewhat surprising that $melH_6$ has to-date attracted very limited interest from the community of magnetic coordination polymer chemists. A search of the literature reveals very few examples of coordination solids prepared using transition metals: these include a low-dimensional, highly hydrated Co(II) polymer,[13a] a 2D Ni(II)-containing material that exhibits very weak antiferromagnetic exchange,[13b] a pillared 3-dimensional (3D) net with Cu(II) and 4,4′-bipyridine,[13c] and a Ag(I)/Mg(II) layered material.[13d] In addition, there exist a handful of structural reports of Ln(III)-mel^{6-} networks (Ln = La,[14a] Ce,[14b] Eu,[14b] Gd(III),[14c,d] Er(III),[14e] Tm,[14a] and Yb.[14b]). A fundamental theme in common with all of these previous examples is the large range of coordination modes observed between metals and mel^{6-} anion.

The mellitate hexaanion, mel^{6-} (Scheme 1a), is subject to considerable steric clashing, owing to the close proximity of neighboring carboxylate groups. This has important repercussions to the way in which mel^{6-} behaves as an organic linker in the formation of metal-organic polymeric arrays. Specifically, one or more of the CO_2^- moieties are forced to rotate out of the aromatic ring plane and are reoriented pseudo-perpendicular to the plane of the parent ring. (Two adjacent CO_2 moieties cannot be coplanar with the C_6 ring. This forces either most of the groups to be somewhat distorted or alternating groups to be pseudo-perpendicular) The ensuing removal of steric repulsion comes at the expense of overall loss of π-conjugation throughout the ligand. The most important consequence from a synthetic viewpoint is that such ligands may behave as truly 3D organic linkers via the formation of (−M−OCO−M−) bridges that are both parallel *and* perpendicular to the same aromatic ring plane. (Scheme 1b) This greatly increases the likelihood that coordination polymers formed using these ligands will preferentially exhibit 3D connectivity, while layered 2D materials are disfavored. This particular structural feature has also been observed previously, in coordination polymers that are based on related aromatic polycarboxylates with adjacent carboxylate groups such as benzene 1,2,4-tricarboxylate,[15] benzene 1,2,4,5-tetracarboxylate,[16] and 2,3-pyridine dicarboxylate.[17]

In the case of the very sterically stressed mel^{6-}, such structural effects are highly pronounced because of the out-of-plane rotation of multiple CO_2^- groups; this in turn results in the possible formation of a number of puckered 7-membered chelate ring modes between octahedral transition metal(II) ions and mel^{6-} (Scheme 2), in addition to the usual range of combinations of *syn*/*anti* bridging modes that are commonly observed for carboxylate.[2,3,11−17] The *bis*- and *tetrakis*-chelate modes (Scheme 2a and 2b respectively) have been observed previously,[13a−c,14a−14c,14e,18] while other highly symmetric modes such as *tris*-chelated mel^{6-} (Scheme 2c) are also hypothetically possible, although not yet observed to the best of our knowledge. All of these chelate modes may be accompanied, in addition, by various combinations of single atom-*O* bridges to

(8) David, W. I. F.; Harrison, W. T. A.; Gunn, J. M. F.; Moze, O.; Soper, A. K.; Day, P.; Jorgenson, J. D.; Hinks, D. G.; Beno, M. A.; Soderholme, L.; Capone, D. W.; Schuller, I. K.; Segre, C. U.; Zhang, K.; Grace, J. D. *Nature* **1987**, *327*, 310.

(9) de la Cruz, C.; Huang, Q.; Lynn, J. W.; Li, J.; Ratcliff, W.; Zarestky, J. L.; Mook, H. A.; Chen, G. F.; Luo, J. L.; Wang, N .L.; Dai, P. *Nature* **2008**, *453*, 899.

(10) (a) Kivelson, S. A.; Yao, H. *Nat. Mater.* **2008**, *7*, 927. (b) Pratt, D. K.; Tian, W.; Kreyssig, A.; Zarestky, J. L.; Nandi, S.; Ni, N.; Bud'ko, S. L.; Canfield, P. C.; Goldman, A. I.; McQueeney, R. J. *Phys. Rev. Lett.* **2009**, *103*, 087001. (c) Christianson, A. D.; Lumsden, M. D.; Nagler, S. E.; MacDougall, G. J.; McGuire, M. A.; Sefat, A. S.; Jin, R.; Sales, B. C.; Mandrus, D. *Phys. Rev. Lett.* **2009**, *103*, 087002.

(11) (a) Cheng, X. N.; Xue, W.; Zhang, W. X.; Chen, X. M. *Chem. Mater.* **2008**, *20*, 5345. (b) Wang, X. Y.; Sevov, S. C. *Chem. Mater.* **2007**, *19*, 3763. (c) Zheng, Y. Z.; Zhang, Y. B.; Tong, M. L.; Xue, W.; Chen, X. M. *Dalton Trans.* **2009**, *14*, 1396. (d) Arora, H.; Lloret, F.; Mukherjee, R. *Eur. J. Inorg. Chem.* **2009**, *22*, 3317. (e) Humphrey, S. M.; Alberola, A.; Gomez Garcia, C. J.; Wood, P. T. *Chem. Commun.* **2006**, 1607. (f) Carballo, R.; Covelo, B.; El Fallah, M.; Ribas, J.; Vasquez-Lopez, E. M. *Cryst. Growth Des.* **2007**, *7*, 1069.

(12) (a) Vilminot, S.; André, G.; Bourée-Vigneron, F.; Baker, P. J.; Blundell, S. J.; Kurmoo, M. *J. Am. Chem. Soc.* **2008**, *130*, 13490. (b) Vilminot, S.; André, G.; Richard-Plouet, M.; Bourée-Vigneron, F.; Kurmoo, M. *Inorg. Chem.* **2006**, *45*, 10938.

(13) (a) Cui, J. C. *Acta Crystallogr.* **2005**, *E61*, m2209. (b) Kumagai, H.; Oka, Y.; Akita-Tanaka, M.; Inoue, K. *Inorg. Chim. Acta* **2002**, *332*, 176. (c) Yang, E.; Zhang, J.; Li, Z. J.; Gao, S.; Kang, Y.; Chen, Y. B.; Wen, Y. H.; Yao, Y. G. *Inorg. Chem.* **2004**, *43*, 6525. (d) Kyono, A.; Kimata, M.; Hatta, T. *Inorg. Chim. Acta* **2004**, *357*, 2519.

(14) (a) Chui, S. S. Y.; Siu, A.; Feng, X.; Zhang, Z. Y.; Mak, T. C. W.; Williams, I. D. *Inorg. Chem. Commun.* **2001**, *4*, 467. (b) Wu, L. P.; Munakata, M.; Suenaga, Y. *Inorg. Chim. Acta* **1996**, *249*, 183. (c) Li, Z. F.; Wang, C. X.; Wang, P.; Zhang, Q. H. *Acta Crystallogr.* **2006**, *E62*, m914. (d) Taylor, K. M. L.; Jin, A.; Lin, W. *Angew. Chem., Int. Ed.* **2008**, *47*, 7722. (e) Deluzet, A.; Guillou, O. *Acta Crystallogr.* **2003**, *C59*, m277.

(15) (a) Xu, X.; Ma, Y.; Lu, Y.; Wang, E.; Bai, X. *J. Mol. Struct.* **2007**, *828*, 68. (b) Lyszczek, R.; Mazur, L.; Rzaczynska, Z. *Inorg. Chem. Commun.* **2008**, *11*, 1091. (c) Lu, Z. L.; Chen, W.; Xu, J. Q.; Zhang, L. J.; Pan, C. L.; Wang, T. G. *Inorg. Chem. Commun.* **2003**, *6*, 244.

(16) (a) Gutschke, S. O. H.; Price, D. J.; Powell, A. K.; Wood, P. T. *Eur. J. Inorg. Chem.* **2001**, *11*, 2739. (b) Chowdhuri, D. S.; Rana, A.; Bera, M.; Zangrando, E.; Dalai, S. *Polyhedron* **2009**, *28*, 2131. (c) Akhbari, K.; Morsali, A. *Inorg. Chim. Acta* **2009**, *362*, 1692; d)

(17) (a) Patrick, B. O.; Stevens, C. L.; Storr, A.; Thompson, R. C. *Polyhedron* **2003**, *22*, 3025. (b) Sileo, E. E.; Vega, D.; Baggio, R.; Garland, M. T.; Blesa, M. A. *Aust. J. Chem.* **1999**, *52*, 205. (c) Gutschke, S. O. H.; Slawin, A. M. Z.; Wood, P. T. *Chem. Commun.* **1995**, 2197. (d) Yu, Z. T.; Li, G. H.; Jiang, Y. S.; Xu, J. J.; Chen, J. S. *Dalton Trans.* **2003**, 4219. (e) Zhang, H. T.; Chen, Y. Q.; Xu, L.; You, X. Z. *Acta Crystallogr.* **2003**, *C59*, m373–m375.

(18) Humphrey, S. M.; Ph.D. Thesis, University of Cambridge, U.K., **2005**.

Scheme 2. Multiple Chelate Modes between mel^{6-} and 3d M(II) Ions: (a) 1,4-bis(chelate);[13a−c,14a−c,e,18] (b) 1,2,4,5-tetrakis(chelate)[18] (c) 1,3,5-*tris*(chelate); (d) the Complete M-mel Coordination Mode As Observed in Compounds **1a**−**c** and **2a**−**c** Presented Herein

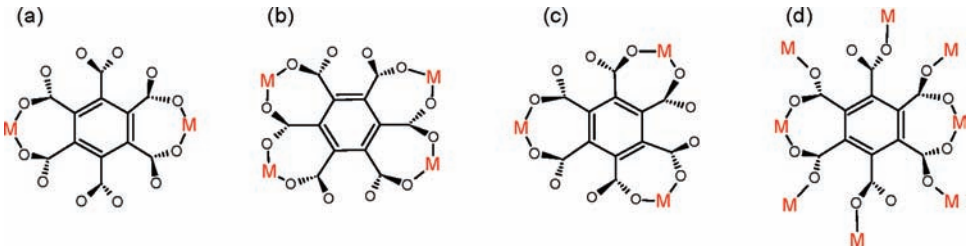

neighboring metals (Scheme 2d). In this paper, the synthesis and magnetic properties of a family of isostructural 3D mellitate-based coordination polymers are presented. These support infinite 2D hexagonal magnetic nets of 3d-M(II) cations; the observed network topology is based on a highly coupled variation of the *bis*-chelated mode (Scheme 2d).

2. Results and Discussion

(a). Synthesis and Structure. In our initial synthetic studies, deprotonation of $melH_6$ with stoichiometric amounts of aqueous KOH gave the intermediate K_6(mel), which was mixed directly with aqueous solutions of a range of transition metal dichlorides ($M'Cl_2$; M′ = Mn, Fe, Co, Ni, Cu, Zn). The resulting viscous slurries were heated to 473 K for 15 h and cooled slowly. In the case of Mn, Co, and Ni, clean crystalline products corresponding to a single phase were obtained, and subsequent single crystal X-ray analysis revealed the products to be isostructural coordination polymer materials, based on the repeat unit, $K_2[M'_2(mel)]$ (M′ = Mn (**1a**); Co (**1b**); Ni (**1c**); Figure 1). A comprehensive series of further reactions were attempted to provide routes to the Fe, Cu, and Zn analogues using alternative precursors, reaction stoichiometries, and synthesis conditions. Unfortunately, isolable analogues were not obtained. However, reactions using alternative alkali metal hydroxides (M = Li, Na, Rb, Cs) under otherwise identical conditions as those used to generate **1a**−**c** enabled easy access to a second isostructural set of compounds of formula, $Rb_2[M'_2(mel)]$ (M′ = Mn (**2a**); Co (**2b**); Ni (**2c**)). The apparent ease with which K could be substituted with Rb to yield isostructural networks can be ascribed to their similar cationic radii (K^+ = 1.33, Rb^+ = 1.48 Å).[19] Meanwhile, reactions employing the other common alkali metals (Li^+ = 0.68, Na^+ = 0.98, Cs = 1.67 Å)[19] afforded a number of related products which exhibit unique network types (not discussed here).

As an example of the structure of the family of compounds **1a**−**c** and **2a**−**c**, the single crystal X-ray data for the K/Mn analogue, $K_2[Mn_2(mel)(OH_2)_2]$, (**1a**) is presented in Figure 1. The material, which crystallizes in the space group $P2_1/n$ (Z = 2), has its aromatic ring bisected by a mirror plane, so that the asymmetric unit is defined as $K[Mn(C_3(CO_2)_3)(OH_2)]$. Thus, twice the asymmetric unit of **1a** constitutes a complete mel^{6-} ligand in which all carboxylate groups are significantly rotated out-of-the-plane of the parent ring (Figure 1a): the torsion angles subtended by the carboxylate groups labeled O1−C4−O2, O3−C5−O4, and O5−C6−O6 are 68.3(3)−72.0(3), 52.9(3)−53.0(4), and 58.1(3)−62.2(3)°, respectively. The donor set around each unique *pseudo*-octahedral Mn(II) ion (bond angles 82.05(8)−99.97(8)°) is provided by five carboxylate-*O* atoms, and a single, terminal OH_2 ligand. Thus, each Mn1 is a 5-connected node within the coordination polymer, and is itself connected to four equivalent mel^{6-} ligands, including a single chelating mode. The ligand hexaanion, mel^{6-} is *bis*-chelated, and the substantial puckering that is required to accommodate the 7-membered chelate rings is facilitated by the out-of-plane orientations of the carboxylate groups. All carboxylate-*O* atoms are coordinated to a single symmetry equivalent Mn1 center with the exception of O5, such that in total, each mel^{6-} is coordinated to eight Mn(II) ions. Of particular note with respect to the magnetic behavior, four of the six carboxylate groups mediate *syn,anti*-bridges between adjacent metal sites (bonds that mediate magnetic exchange pathways are drawn in green in Figure 1a). The framework building block, $[M'_2(mel)(OH_2)_2]^{2-}$, results in a highly connected 3D anionic coordination polymer material.

A projection of the extended lattice of **1a** in the crystallographic *bc*-plane (Figure 1b) reveals small channels within the structure that are occupied by the alkali metal counterions. Since there is no solvent of crystallization present in the lattice, the K^+ ions (or Rb^+ ions for **2a**−**c**) form their closest contacts with coordinated OH_2 ligands that project into the same cavities (K···O = 2.691(2) Å), and to the lone uncoordinated carboxylate-O5 (K···O = 2.747(2) Å). The ligand aromatic rings are arranged in an approximate herringbone array, and serve to link between adjacent metal-carboxylate sheets; this provides substantial separation between adjacent magnetic layers. Consideration of the metal-carboxylate magnetic lattice with all aromatic portions omitted reveals infinite hexagonal networks that are composed of fused $[\text{-M-(OCO)-}]_6$ rings that are arranged in a brick-weave motif (Figure 1c). When the sheets are viewed end-on along the *ac*-bisector, they can be seen to gently undulate and are separated by interstitial layers of alkali metal cations (Figure 1d).

Further investigations of the chemistry of $melH_6$ with alternate metal precursors and variable reaction pH led to the discovery of a third isostructural Co(II)-containing material that was prepared using aqueous hexamine cobalt(III) chloride. Crystalline material obtained from reactions at 513 K over longer reaction times (24−48 h) was found to have the composition, $(NH_4)_2[Co_2(mel)(OH_2)_2]$ (**3**). Polymer **3** is directly analogous to **1b** and **2b**, albeit with the replacement of all alkali metal ions with NH_4^+. This is noteworthy from a synthetic perspective, in that the anionic framework topology, $[M(mel)(OH_2)_2]^{2-}$, as observed in the above materials appears to be highly favorable in the presence of counterions of appropriate size. Figure 2 shows a section of the structure of **3** that details the position of a single NH_4^+ moiety within a pore; a network of short-range intermolecular (N···O)

(19) Collin, R. J.; Smith, B. C. *Dalton Trans.* **2005**, 702.

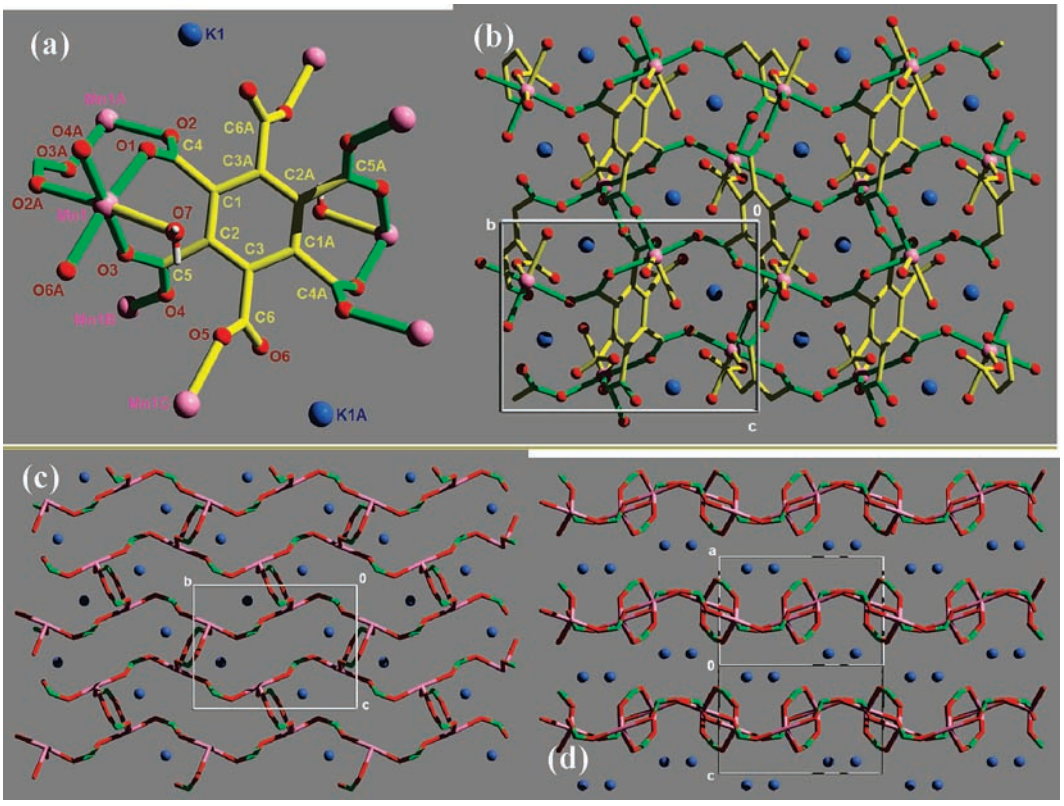

Figure 1. (a) Twice the asymmetric unit of **1a**, showing the completed coordination environment around a single mel^{6-} ligand (magnetic superexchange pathways are drawn as green bonds); (b) the extended structure of **1a** viewed normal to the *a*-axis; (c) the magnetic lattice also normal to *a*, with all aromatic rings omitted for clarity; (d) view in the *ac*-bisector, showing adjacent 2D magnetic hexagonal net layers, with interstitial alkali metal ions.

distances (2.71, 2.74, 2.90, 3.15 Å) are formed between each NH_4^+ and surrounding carboxylate and coordinated OH_2 groups.

(b). Magnetism. The magnetic susceptibility has been measured for all compounds, **1a**−**c**, **2a**−**c**, and **3**. An exponential increase in χ is observed in **1b**, **1c**, **2b**, and **2c**, while the K/Mn analogue (**1a**) shows a maximum at approximately 8 K, for the corresponding Rb/Mn (**2a**), there is a reduction in the gradient of the curve. None of the materials show any indication of long-range ordering down to 5 K. The results obtained by fitting of the inverse susceptibility for all compounds to the Curie−Weiss law are summarized in Table 1. Using the definition of the Curie constant (eq 1),

$$C = \frac{Ng^2\mu_B^2 S(S+1)}{3k_B} \qquad (1)$$

it is possible to estimate the *g* factor. This relies on the assumption that in all cases, the transition metal ions have good spin quantum numbers, which for Ni(II) and Mn(II) is a good approximation. The obtained *g* value for **1a** is anomalously low, although all normal checks (i.e., comparison of the fitted *C* value with the room temperature value of χT; Table 1) indicate that the data is actually well-behaved and satisfactory. All other *g* factors are within the ranges expected. The situation for cobalt containing phases is slightly more complicated as the spin only approximation is not valid because of the unquenched orbital angular momentum. However, assuming that there is no orbital contribution and $S = 3/2$, the value of *g* is within the range previously reported using this approximation.[20]

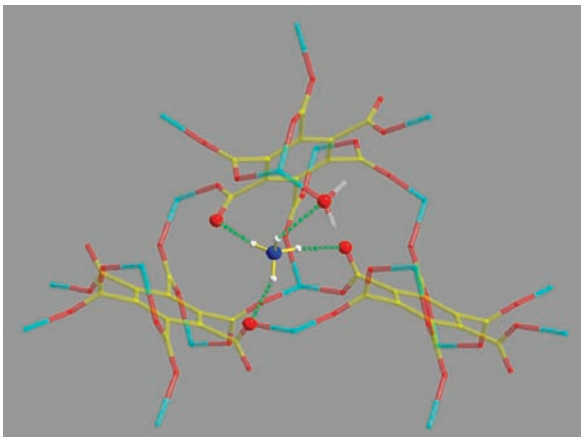

Figure 2. Structure of isostructural **3** showing NH_4^+ cations and close-range N−H···O contacts within the pores.

Analysis of the Weiss constant (Θ) allows for the determination of the predominant exchange interactions within each system. In the case of the Mn(II)- and Ni(II)-based materials (**1a**, **1c**, **2a**, and **2c**) there is negligible orbital contribution to the magnetic moment, and the sign of the Weiss constant is a direct indication of the nature of the exchange interactions; therefore, antiferromagnetic interactions are expected to dominate for Mn-containing **1a** and **2a**, while ferromagnetic exchange

(20) Carlin R. L. *Magnetochemistry*; Springer: Berlin, Germany, 1986.

Table 1. Parameters Obtained from Susceptibility Data

	C_{meas} (cm^3 mol^{-1} K)	Θ (K)	g_{calc} [a]	g_{HT} [b]	J_{Weiss} (K)	J_{HT} (K)
1a	3.799(3)	−14.2(1)	1.87	1.851(1)	−0.81	−0.655(4)
2a	4.645(9)	−8.3(2)	2.06	2.055(1)	−0.474	−0.434(3)
1c	1.209(1)	1.2(2)	2.20	2.180(4)	0.30	0.42(1)
2c	1.28(2)	0.6(2)	2.35	2.32(1)	0.15	0.49(3)
1b	3.61(1)	−23.6(5)	2.78		−3.15	
2b	3.81(1)	−24.3(6)	2.85		−3.24	
3	3.39(2)	−24.8(6)	2.69			

[a] See eq 1. [b] See eqs 4 and 5.

interactions are expected to dominate in the corresponding Ni phases, **1c** and **2c**. For **1b**, **2b**, and **3** (containing Co(II)) the issue is somewhat more complicated as in an octahedral field the $^4T_{1g}$ ground term is split by the effect of spin−orbit coupling. This produces a manifold consisting of (in order of increasing energy) $J' = 1/2, 3/2, 5/2$ states. As the spin−orbit coupling constant is relatively small in this case, the population of the ground state increases rapidly as the temperature decreases, resulting in a negative contribution to the Weiss constant. This contribution is typically small, and the large negative values observed for the Co(II) phases are still consistent with predominantly antiferromagnetic interactions.

Structural considerations allow us to account for the observed magnetic behavior; typically the shortest superexchange pathways mediate the strongest spin−spin interactions. In the structure of **1a**−**c**, **2a**−**c**, and **3** two distinct superexchange pathways result in the formation of distorted hexagonal nets: (a) single *syn,anti*-carboxylate bridges that form infinite chains (Figure 3, dashed red bonds); and (b) double *syn,anti*/*anti,syn*-carboxylate bridges that connect between adjacent *syn,anti* chains (Figure 3, dashed cyan bonds). To avoid over-parameterization of data based on this simple model, as a first approximation it can be assumed that both types of bridges provide exchange interactions, *J*, of identical strength. The 2D hexagonal net layers are separated by the conjugated aromatic rings, and these pathways are anticipated to provide negligible superexchange; the interlayer distance is 4.48 Å (M···M) and should result in very weak dipolar coupling.

At the simplest level we can apply Weiss's mean field theory (MFT) to the measured Weiss constant to estimate *J*. If the Heisenberg−Dirac−Van Vleck Hamiltonian is defined as shown in eq 2,

$$\hat{H} = -2\sum_{ij} J_{ij}\hat{S}_i \cdot \hat{S}_j \qquad (2)$$

where the summation is over all exchange interactions in the honeycomb lattice, the appropriate form of MFT is then given by eq 3

$$\Theta = \frac{2S(S+1)zJ}{3k_B} \qquad (3)$$

where *z* is the number of nearest neighbors; for the honeycomb lattice (Figure 2), $z = 3$. A first estimate of the coupling constants may be made using eq 3; these are

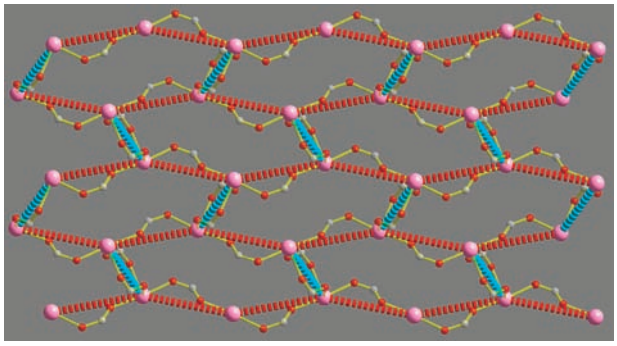

Figure 3. Hexagonal (honeycomb) lattice of 3d M(II) ions present in **1a**−**c**, **2a**−**c**, and **3**. The carboxylate bridges are shown with yellow bonds; thick dashed red lines represent superexchange pathways mediated by single *syn,anti*-bridges; thick dashed cyan lines show the double *syn,anti*-bridges.

listed in Table 1. This is certainly a very crude approach as it neglects the structural anisotropy of the exchange lattice, although it is useful to provide a magnitude for the coupling. The high temperature series expansions for both antiferromagnetic and ferromagnetic lattices for a general spin *S*, on a general lattice, have been developed by Rushbrooke and Wood.[21] The coefficients of this expansion have been calculated for varying 2D lattices including the Heisenberg square lattice[22] and the honeycomb lattice[23] and are frequently used to extract exchange coefficients from the high temperature, paramagnetic, region of the susceptibility curve. The expression per metal ion for a system with ferromagnetic exchange interactions is given in eq 4, while that of the antiferromagnetic case is given in eq 5.

$$\chi = \frac{Ng^2\mu_B^2 S(S+1)}{3k_B T} \frac{1}{1+\sum_i b_i \left(\frac{J}{kT}\right)^i} \qquad (4)$$

$$\chi = \frac{Ng^2\mu_B^2 S(S+1)}{3k_B T} \frac{1}{1+\sum_i (-1)^i b_i \left(\frac{J}{kT}\right)^i} \qquad (5)$$

Here, $x = |J|/kT$, where *J* is the exchange interaction. The coefficients, b_n, for Mn^{2+} and Ni^{2+} are listed in Table 2.

The susceptibility data for **1a**, **1c**, **2a**, and **2c** were rescaled for one magnetic atom and fitted to the appropriate form of the series expansion (Figures 4−7 respectively). In all cases, data were fitted accurately in the high temperature region (50−300 K). Because of the nature of the technique, it is anticipated that very low temperature data

(21) Rushbrook, G. S.; Wood, P. J. *Mol. Phys.* **1958**, *1*, 257.
(22) (a) Tsirlin, A. A.; Belik, A. A.; Shpanchenko, R. V.; Antipov, E. V.; Takayama-Muromachi, E.; Rosner, H. *Phys. Rev. B.* **2008**, *77*, 092402. (b) Manson, J. L.; Conner, M. M.; Schlueter, J. A.; Lancaster, T.; Blundell, S. J.; Brooks, M. L.; Pratt, F. L.; Papageorgiou, T.; Bianchi, A. D.; Wosnitza, J.; Whangbo, M.-H. *Chem. Commun.* **2006**, 4894.
(23) (a) Joy, P. A.; Vasudevan, S. *Phys. Rev. B.* **1992**, *46*, 5425–5433. (b) Clement, R.; Girerd, J. J.; Morgenstern-Badarau, I. *Inorg. Chem.* **1980**, *19*, 2852. (c) Viciu, L.; Huang, Q.; Morosan, E.; Zandbergen, H. W.; Greenbaum, N. I.; McQueen, T.; Cava, R. J. *J. Solid State Chem.* **2007**, *18*, 1060. (d) le Flem, G.; Brec, R.; Ouvard, G.; Louisy, A.; Segransan, P. *J. Phys. Chem. Solids* **1982**, *43*, 455. (e) Rogado, N.; Huang, Q.; Lynn, J. W.; Ramirez, A. P.; Huse, D.; Cava, R. J. *Phys. Rev. B.* **2002**, *65*, 144443.

Table 2. Coefficients, *b*

	$S = 1$	$S = 5/2$
b_1	−4	17.5
b_2	7.333	110.833
b_3	−7.111	304.111
b_4	−5.703	991.828
b_5	22.281	9346.14
b_6	51.737	264381.31

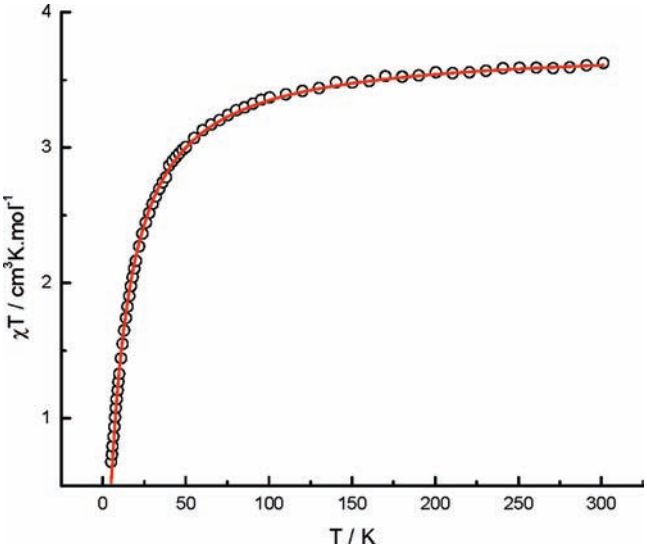

Figure 4. Susceptibility data (open circles) and fit (red line) for **1a**.

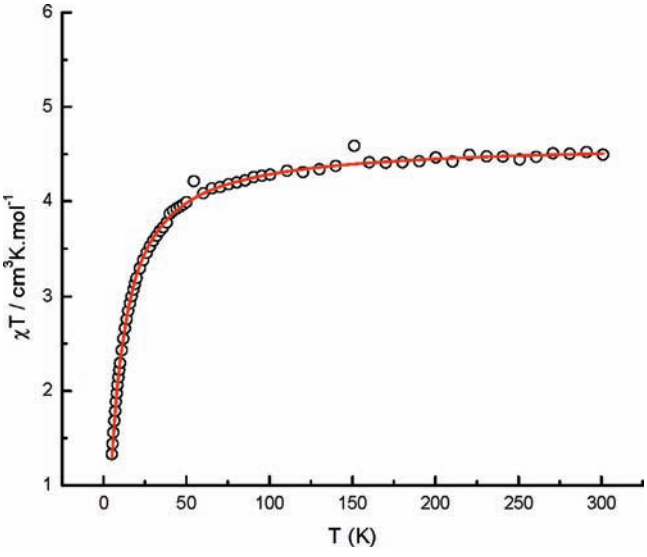

Figure 5. Susceptibility data (open circles) and fit (red line) for **1c**.

cannot be as accurately described using the series expansion approach employed. The results of this fitting procedure are displayed in Table 1. The values of the exchange interactions obtained are within the range of those previously observed for *syn,anti*-carboxylate bridges for Mn(II)[24] and Ni(II),[25] respectively. The only unusual result of this investigation is the relatively low values of

(24) Gutschke, S. O. H.; Price, D. J.; Powell, A. K.; Wood, P. T. *Inorg. Chem.* **2000**, *39*, 3705.
(25) Yoneda, K.; Masaaki, O.; Shiga, T.; Oshio, H.; Kitagawa, S. *Chem. Lett.* **2007**, *36*, 1184.

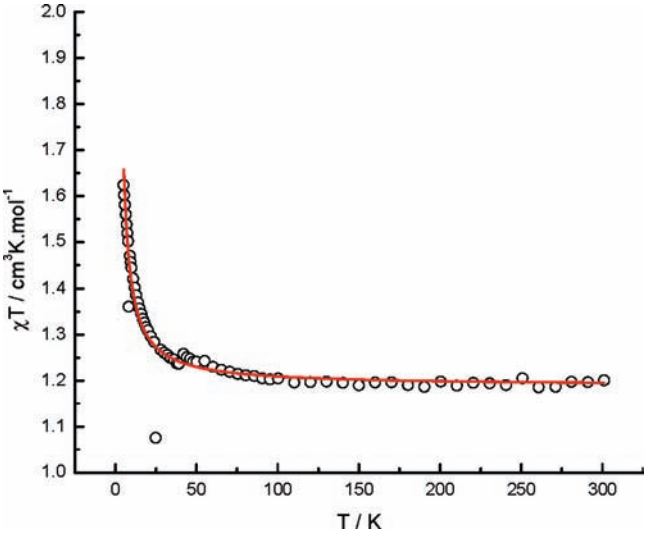

Figure 6. Susceptibility data (open circles) and fit (red line) for **2a**.

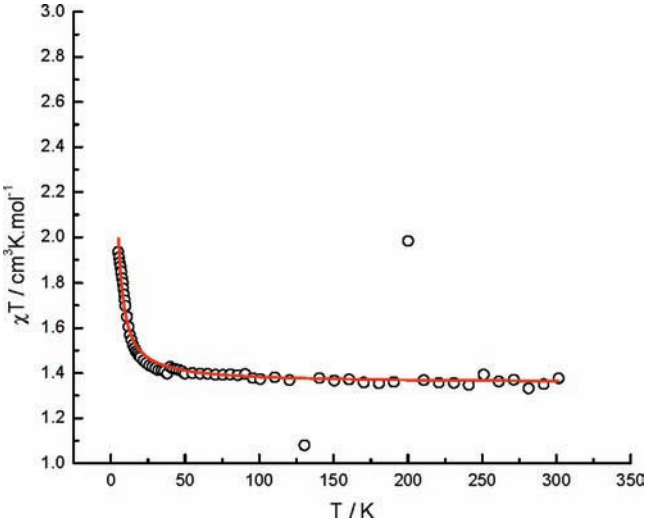

Figure 7. Susceptibility data (open circles) and fit (red line) for **2c**.

g that were obtained for the potassium containing phases, **1a** and **1c**. Because of the complexity of the analysis required, similar modeling has not been extended to include the Co(II)-containing phases. Comparative susceptibility data for the Co(II) phases, **1b** (K/Co) and **2b** (Rb/Co), are shown in Figure 8.

3. Conclusions

A family of isostructural organic−inorganic coordination materials have been prepared using the 1,2,3,4,5,6-benzene hexacarboxylate hexaanion, mel^{6-}. Out-of-aromatic-plane rotation of adjacent carboxylate groups is a defining feature of mel^{6-}, which makes it an ideal organic building block for the formation of low-symmetry coordination polymers with high metal-to-ligand connectivity. The favorable structural type presented herein is based on honeycomb (hexagonal) magnetic nets of paramagnetic transition metal-carboxylate sheets, which are effectively isolated from each other by interstitial layers of aromatic organic moieties and alkali metal ions that are resident within structural cavities. These materials have presented an ideal opportunity to apply the

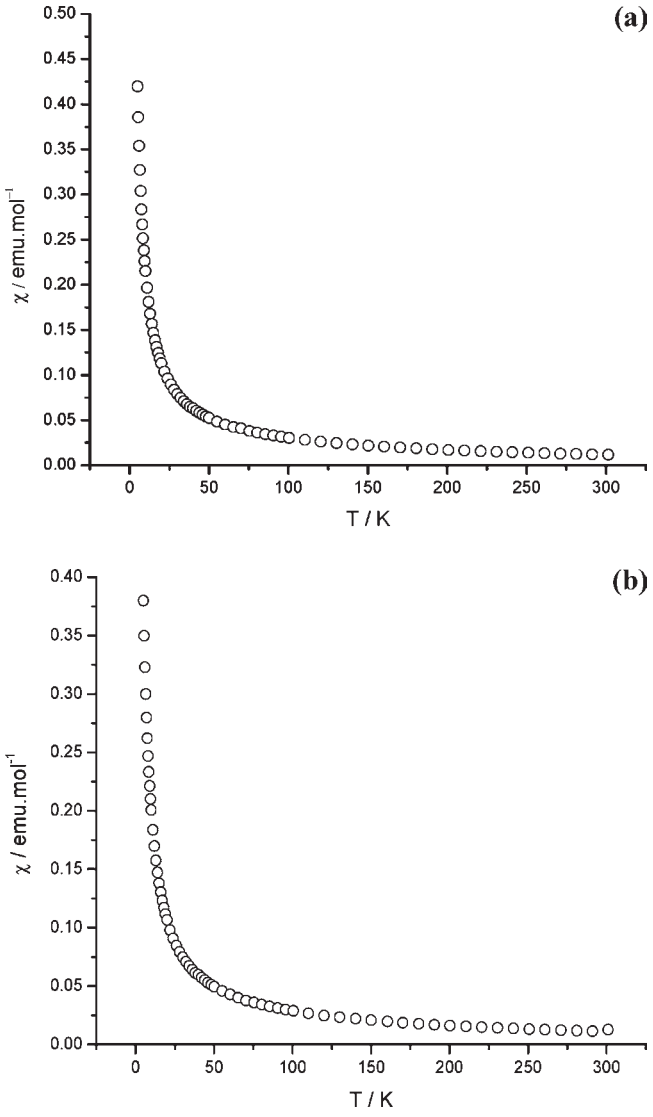

Figure 8. (a) Susceptibility data for **1b**. (b) Susceptibility data for **2b**.

known model for isolated hexagonal magnetic nets to previously unstudied "real" examples. It has been shown that the observed temperature-dependent magnetic susceptibility of Mn(II)- and Ni(II)-based versions are in very close agreement with this mode. In addition, the identity of the alkali metal ions that are incorporated within the structures has an indirect effect on the comparative susceptibilities.

4. Experimental Section

X-ray Crystallography. Crystals were mounted on thin glass fibers using perfluoropolyether oil, which was frozen in situ by the cold nitrogen gas Cryostream flow. Data for compounds **1a**, **2a**, and **3** were collected using an Enraf Nonius Kappa CCD diffractometer using monochromated Mo Kα radiation (λ = 0.71073 Å). Cell refinement and data reduction was performed using the HKL SCALEPACK & DENZO[26] and COLLECT[27] utilities. Absorption corrections were made based on ψ- and ω-scans using the SORTAV program.[28] Structures were solved using direct methods and refined on F^2 using the program SIR-92[29] and then refined using the SHELXTL-97 software.[30] All non-hydrogen atoms were refined anisotropically for all structures. H-atoms belonging to coordinated OH_2 and to NH_4^+ were directly located in the peak difference maps and allowed to refine freely. Further information for the structures **1a**, **2a**, and **3** is given in Table 3.

SQUID Magnetometry. All DC susceptibility data were measured on homogenized crystalline samples using a Quantum Design MPMS-5 magnetometer. Temperature scans were recorded in the range 5−300 K with an external applied field of 100 G and isothermal magnetization was recorded at 5 K in the range ± 50 kG (±5.0 T). The data were corrected for diamagnetism using Pascal's constants.[31]

General Procedure. $MnCl_2 \cdot 4H_2O$ (Lancaster), $CoCl_2 \cdot 6H_2O$ (Avocado), KOH, RbOH (50% solution in water), and $NiCl_2 \cdot 6H_2O$ (Aldrich) were used as received. Mellitic acid was purchased from Fluka and used as received. Stock solutions of 1.00 M M′OH (M′ = K, Rb) were prepared in volumetric flasks and stored at 298 K.

All reaction mixtures had a total solution volume of 6.5 cm^3 ± 0.5 cm^3 and were heated in 23.0 cm^3 Teflon-lined autoclaves, purchased from the Parr Corp., Illinois. Conventional insulated box ovens and armored tube furnaces fitted with thermocouple temperature control devices were used to heat all reactions. Infrared spectra of solid-phase products, compressed into disks using a matrix of KBr, were measured in the range 40000−400 cm^{-1} with a Perkin-Elmer RXI FT-IR spectrophotometer. Emission spectra were recorded by diffuse reflectance from powdered analytes on a Perkin-Elmer Lambda 12 UV/vis spectrophotometer fitted with Labsphere RSA-PE-20 reflectance apparatus. C, H, N microanalysis data were collected by the in-house service.

Synthesis. In all cases the generic abbreviation M:L:OH:M′ describes the stoichiometric ratios of principal metal M, ligand L, base OH and secondary metal M′ (mineralizing agent) where used.

$K_2[M_2(mel)(OH_2)_2]$ (M = Mn, (1a); Co, (1b), Ni (1c)). Mellitic acid (68 mg, 0.20 mmol) was dissolved in H_2O (2.0 cm^3) and KOH (1.0 M, 1.2 cm^3) was added. The solution was stirred and a second solution of MCl_2 (M = Mn (**1a**), 80 mg, 0.40 mmol; M = Co (**1b**), 95 mg, 0.40 mmol; M = Ni (**1c**), 95 mg, 0.40 mmol) in H_2O (3.3 cm^3) was added to give a ratio of 2:1:6. The solution was heated for 15 h at 473 K and cooled over a further 5 h. Crystalline material was separated from white homogeneous powder by short cycles of sonication (3 × 10 s) and washing with H_2O.

$K_2[Mn_2(mel)(OH_2)_2]$ (**1a**), colorless square plates (yield 81 mg, 72%). Anal. Found: C, 25.3; H, 0.87. $C_{12}H_4K_2Mn_2O_{14}$ requires: C, 25.7; H, 0.72. ν_{max} (KBr/cm^{-1}): 3353 m br, 3394 m br, 1651 s, 1629 s, 1587 s, 1560 s, 1447 s, 1431 s, 1411 s, 1347 s, 1328 s, 1188 m, 916 m, 901 m, 810 w, 790 w, 772 w, 715 m, 695 m.

$K_2[Co_2(mel)(OH_2)_2]$ (**1b**), dark pink square plates (yield 84 mg, 74%). Anal. Found: C, 25.0; H, 0.95. $C_{12}H_4K_2Co_2O_{14}$ requires: C, 25.4; H, 0.71. λ_{max} (powder/nm): 532(0.25), 496(0.23), 475(0.20). ν_{max} (KBr/cm^{-1}): 3354 m, 3393 m br, 1636 s, 1592 s, 1560 s, 1447 s, 1436 s, 1411 m, 1349 s, 1330 s, 1189 m, 917 m, 901 m, 803 w, 799 w, 701 m, 648 m br, 589 m, 530 m.

$K_2[Ni_2(mel)(OH_2)_2]$ (**1c**), light green square plates (yield 89 mg, 78%). Anal. Found: C, 25.0; H, 0.97. $C_{12}H_4K_2Ni_2O_{14}$ requires: C, 25.4; H, 0.71. λ_{max} (powder/nm): 742(0.14), 680(0.14), 410(0.39). ν_{max} (KBr/cm^{-1}): 3546 m, 3386 m, 1686 m, 1655 s, 1638 s, 1618 s, 1560 s, 1508 m, 1490 w, 1438 s, 1411 m, 1350 s, 1330 s, 1189 m, 919 m, 903 m, 806 w, 732 w, 773 w, 717 m, 704 m, 670 m, 626 m, 592 m, 536 m.

(26) *HKL SCALEPACK*; Otwinowski, Z.; Minor, W. In *Methods in Enzymology, Macromolecular Crystallography*; Carter, C. W., Jr., Sweet, R. M., Eds.; Academic Press: New York, 1997; Vol. *276*, Part A, p 307.
(27) *COLLECT*; Nonius BV: Delft, The Netherlands, 1997−2002.
(28) *SORTAV*; Blessing, R. H. *Acta Crystallogr.* **1995**, *A51*, 33.
(29) Altamore, A.; Burla, M. C.; Camalli, G.; Cascarano, G.; Giacovazzo, C.; Gualiardi, A.; Polidori, G. *J. Appl. Crystallogr.* **1994**, *27*, 435.
(30) Sheldrick, G. M. *SHELXTL*, Version 6.10; Bruker AXS Inc: Madison, WI, 1997.
(31) Kahn, O. *Molecular Magnetism*; Wiley-VCH: New York, 1993.

Table 3. Crystal Data

identifier	1a	2a	3
chemical formula	$C_{12}H_4K_2Mn_2O_{14}$	$C_{12}H_4Mn_2O_{14}Rb_2$	$C_{12}H_{12}Co_2N_2O_{14}$
crystal habit	parallelepiped	parallelepiped	parallelepiped
crystal system	monoclinic	monoclinic	monoclinic
space group	$P2_1/n$	$P2_1/n$	$P2_1/n$
a (Å)	8.4840(2)	8.5180(5)	8.4267(2)
b (Å)	11.0614(3)	11.1848(2)	10.9735(4)
c (Å)	9.1046(2)	9.1441(5)	9.0131(3)
β (deg)	116.1167(17)	116.511(7)	116.383(2)
V (Å^3)	767.18(3)	789.82(2)	746.64(2)
Z	2	2	2
D_{calcd} (g cm^{-3})	2.425	2.782	2.340
M	560.23	652.96	526.10
$F(000)$	552	700	528
M (Mo−Kα, mm^{-1})	2.277	8.450	2.320
$2\theta_{max}$ (deg)	27.08	27.46	25.00
no. reflections measured	4607	4771	5219
no. unique reflections	1679	1770	1284
R_{int}	0.043	0.045	0.040
$R1^a(F > 4\sigma(F))$	0.033	0.066	0.032
$wR2^b(F^2$, all data)	0.076	0.209	0.069
no. reflections used	1679	1770	1284
no. paramaters	144	142	136
no. restraints	0	3	0
GOF^c	1.031	1.075	1.063
max. $\Delta\rho$ /e·Å^{-3}	−0.45	1.91	0.49

^{a} $R(F) = \sum||F_o| - |F_c||/\sum|F_o|$. ^{b} $wR(F^2) = [\sum w(F_o^2)^2]^{0.5}$; $w^{-1} = \sigma^2(F_o^2) + (aP)^2 + bP$, where $P = [F_o^2 + 2F_c^2]/3$ and a and b are constants adjusted by the program. ^{c} GOF $= [\sum[w(F_o^2 - F_c^2)^2/(n-p)]^{0.5}$, where n is the number of data and p the number of parameters.

$Rb_2[M_2(mel)(OH_2)_2]$ (M = Mn, (2a); Co, (2b), Ni (2c)). As for **1a**−**c**, but using RbOH (1.0 M, 1.2 cm^3) as the base in each case. Crystals were either directly isolated by vacuum filtration and washing with H_2O or were cleaned by short cycles of sonication (3 × 10 s) where necessary.

$Rb_2[Mn_2(mel)(OH_2)_2]$ (**2a**), colorless square plates (yield 56 mg, 43%). Anal. Found: C, 22.3; H, 1.09. $C_{12}H_4Rb_2Mn_2O_{14}$ requires: C, 22.1; H, 0.62. ν_{max} (KBr/cm^{-1}): 3534 m, 3403 m br, 1637 s, 1588 s, 1560 s, 1427 s, 1344 s 1320 s, 1256 m, 1185 m, 911 m, 899 m, 810 w, 770 w, 715 m, 690 m, 586 m.

$Rb_2[Co_2(mel)(OH_2)_2]$ (**2b**), dark pink square plates (yield 52 mg, 39%). Anal. Found: C, 22.3; H, 1.01. $C_{12}H_4Rb_2Co_2O_{14}$ requires: C, 21.8; H, 0.61. λ_{max} (powder/nm): 533(0.55), 308(0.82), 300(0.83), 280(0.89), 216(0.83) ν_{max} (KBr/cm^{-1}): 3546 m, 3393 m br, 1641 s, 1592 s, 1561 s, 1438 s, 1405 m, 1345 s, 1330 m, 1186 m, 913 m, 898 m, 809 w, 716 w, 695 m, 670 w, 590 m, 528 m.

$Rb_2[Ni_2(mel)(OH_2)_2]$ (**2c**), light green square plates (yield 51 mg, 39%). Anal. Found: C, 22.2; H, 1.16. $C_{12}H_4Rb_2Ni_2O_{14}$ requires: C, 21.8; H, 0.71. λ_{max} (powder/nm): 752(0.30), 415(0.55), 306(0.73), 288(0.79), 267(0.78). ν_{max} (KBr/cm^{-1}): 3528 m, 3384 m br, 1648 s, 1613 s, 1560 s, 1438 s, 1406 m, 1344 s, 1330 s, 1185 m, 801 m, 900 m, 807 w, 769 w, 717 m, 698 m, 668 m, 593 m, 526 m.

$(NH_4)_2[Co_2(mel)(OH_2)_2]$ (3). $Co(NH_3)_6Cl_3$ (120 mg, 0.45 mmol) was dissolved in water (8.0 cm^3), and solid mellitic acid was added (100 mg, 0.30 mmol). The resulting slurry was heated at 513 K for 40 h and cooled to room temperature over 8 h. The resulting pink crystalline prisms were collected, washed with H_2O, and dried via vacuum filtration (yield 35 mg, 30%). Anal. Found: C, 27.1; H, 2.4; N, 5.4. $C_{12}H_{12}Co_2N_2O_{14}$ requires: C, 27.4; H, 2.3; N, 5.3%. ν_{max} (KBr/cm^{-1}): 3556 m br, 3211, m br, 2953 w, 1557 s, 1424 s, 1415 s, 1323 s, 1186 w, 913 w, 898 m, 809 w, 769 w, 717 m, 696 m.

Acknowledgment. The authors would like to thank Dr. John E. Davies for assistance with single crystal X-ray studies and the EPSRC for funding.

Supporting Information Available: Additional magnetic susceptibility data and IR spectra. This material is available free of charge via the Internet at http://pubs.acs.org. CCDC reference numbers 751741 to 751743 contain the data for **1a**, **2a**, and **3** respectively; this data is available free-of-charge from www.ccdc.cam.ac.uk.